Reference: *Biol. Bull.* **217:** 253–268. (December 2009)

Unusual Development of the Mitraria Larva in the Polychaete *Owenia collaris*

TRACEY I. SMART[1,*,†] AND GEORGE VON DASSOW[1,2]

[1]*Oregon Institute of Marine Biology, University of Oregon, Charleston, Oregon 97420; and* [2]*Center for Cell Dynamics, Friday Harbor Laboratories, 620 University Rd., Friday Harbor, Washington 98250, and Department of Biology, University of Washington, Seattle, Washington 98195*

Abstract. Despite the wide variety of larval forms among polychaetes, most are clearly derived from the canonical spiralian trochophore. Within the genus *Owenia* (family Oweniidae), however, the mitraria larva lacks the characteristic ciliary bands of the trochophore, and those it has are monociliated, typically a deuterostome characteristic. Adult *Owenia* spp. also possess a monociliated epidermis and deuterostome-like nephridia. This study is the first detailed account of early embryology for any member of the Oweniidae. Light, confocal, and scanning electron microscopy were used to investigate organogenesis from fertilization through metamorphosis in *Owenia collaris*. Equal spiral cleavage yields an embryo with an unusually large blastocoel for a spiralian. The embryo undergoes gastrulation by invagination, and begins swimming 24 h after fertilization. Three important events deviate markedly from stereotypical polychaete embryogenesis. First, at the 8-cell stage the micromeres are larger than the macromeres, as in nemerteans. Second, the blastopore becomes the anus, as in some deuterostomes, while the stomodeum may form secondarily. Third, the cells that would form the prototroch in a canonical spiralian trochophore ($1q^2$ descendants) never undergo cleavage arrest, and the primary ciliated band of the mitraria never contains large, multiciliated cells. The mitraria larva thus represents a mixture of protostome and deuterostome developmental traits, suggesting that spiralian development is not so rigidly constrained as it might appear.

Received 4 May 2009; accepted 21 August 2009.

* To whom correspondence should be addressed. E-mail: tis@u.washington.edu

† Present Address: NOAA Alaska Fisheries Science Center, 7600 Sand Point Way NE, Seattle, WA 98115; and School of Aquatic and Fisheries Science, University of Washington, Seattle, WA 98191.

Introduction

Annelid development is as diverse as the habitats and morphologies of the adult animals. Annelid embryos typically undergo total spiral cleavage and protostomy (Okada, 1970), but they exhibit broad variation on this theme. Eggs may be very yolky and produce stereoblastulae, or they may have little to no yolk and produce coeloblastulae. The mode of gastrulation correlates with the amount of yolk: yolky embryos gastrulate by epiboly; non-yolky embryos by invagination (Okada, 1970). Direct and indirect development, feeding and nonfeeding larvae, and gradual and catastrophic metamorphoses are all manifest among annelids. Among taxa with indirect development, yolky eggs frequently give rise to nonfeeding larvae, whereas non-yolky eggs produce feeding larvae. Most annelid larval forms, feeding or not, can be readily related to the trochophore ground plan, which Nielsen (2001, 2004) defined as a larva bearing an apical tuft, a preoral ciliated band derived from trochoblasts (prototroch), an adoral ciliary zone, and postoral metatroch, gastrotroch, and telotroch, all of which bands consist of multiciliate cells with compound cilia. Based on the lack of homology between the postoral ciliated bands and on recent phylogenies of protostomes and polychaetes, a broader definition of trochophore is more likely to reflect the plesiomorphic condition: a larva with a preoral ciliated band derived from trochoblasts (prototroch) (Damen and Dictus, 1994; Rouse, 1999; Maslakova *et al.,* 2004). In polychaetes, the trochopore undergoes teloblastic growth post-embryonically to form segments from the posterior end (Schroeder and Hermans, 1975). Segments develop sequentially from pockets of mesoderm, which form new coelomic compartments through schizocoely, along with continued elongation of the epiderm.

A few annelid larvae are so highly derived—assuming

that the trochophore in the sense of Rouse (1999) is indeed a plesiomorphic form—that they are not immediately recognizable as manifestations of the trochophore ground plan. These cases are important both embryologically and phylogenetically, because they highlight the adaptability, rather than the conservatism, of the spiralian developmental program. For example, larvae of the species of *Marphysa* discussed by Aiyar have no distinct ciliary bands; instead the whole surface of the larva is ciliated (Aiyar, 1931). It may very well be, however, that the ciliated cells in question are derived from the trochoblast cell lineage, as has been suggested for pericalymma larvae of protobranch bivalve and neomenioid aplacophoran molluscs (Thompson, 1960; Zardus and Morse, 1998), and shown to be the case in the palaeonemertean *Carcinoma tremaphoros* (Maslakova *et al.,* 2004). For another example, the endolarva of *Polygordius appendiculatus* develops the segmented body as an elaborate folded pouch within the highly inflated larval hyposphere, rather than adding segments progressively to the posterior of the post-trochal region (Woltereck, 1902; Okada, 1970; ironically, this unusual larva is the original inspiration for the trochophore concept—see Rouse, 1999). One of the most unusual forms is the mitraria larva of the family Oweniidae. The hyposphere of the mitraria is greatly reduced, and the segmental body develops internal to the larval body as a juvenile rudiment. A remarkable feature of the mitraria is that the apparent homologs of the prototroch, metatroch, and food groove consist of monociliated cells (Emlet and Strathmann, 1994).

D. P. Wilson (1932) first documented larval and juvenile development of *Owenia fusiformis,* demonstrating both the unusual morphology of the mitraria and the unusual metamorphosis of this larva. However, there are no published studies on the early development of *O. fusiformis* or any species within the family Oweniidae that link cleavage and embryogenesis to larval morphology. The current study is an account of embryogenesis and development through the juvenile stage of *Owenia collaris* (Hartman, 1969). Our primary focus was to document the major events in development of this species from fertilization to metamorphosis, with particular attention to cleavage, gastrulation, and formation of the larval ciliary bands and juvenile body. Secondarily, the development through metamorphosis of this species was used to determine whether there are commonalities that can be used to define developmental patterns for the genus *Owenia* or to differentiate species within this genus.

Materials and Methods

Adult *Owenia collaris* were collected from mudflats in the Coos Bay estuary, Oregon, or False Bay, San Juan Island, Washington, during spring and summer in the years 2004–2007, and were taken to either the Oregon Institute of Marine Biology or the Friday Harbor Laboratories. The worms were held separately in 0.45-μm filtered seawater (FSW) at ambient seawater temperatures (10–13 °C) until they spawned naturally. Both sexes released gametes from a pair of posterior pores. If a worm failed to spawn, viable gametes could be obtained by removing it from its tube with fine forceps and piercing holes in the epidermis through which gametes could escape from the coelom.

A few drops of diluted sperm suspension were added to culture dishes containing a monolayer of eggs in 0.45-μm FSW. Cultures were covered and kept in an incubator set at 12 °C. Occasionally polyspermy occurred, but at very low frequencies. Developing embryos and larvae were photographed alive using light microscopy or were fixed for either confocal microscopy or scanning electron microscopy. To improve images, jelly coats were often removed after fertilization by placing eggs into a 1:1 mixture of 0.25 mol l^{-1} NaCitrate: 1 mol l^{-1} sucrose, and then passing fertilized embryos through a 73-μm sieve (Winesdorfer, 1967; Render, 1982). Time-lapse videos were made with a Hamamatsu C2400 CCD video camera mounted on a Zeiss WL standard DIC scope with 40× 0.85 NA water-immersion lens in a temperature-controlled chamber at 12 °C. Images were captured and converted to video using BTV Pro 5.4.1 for Mac OS X (Ben's Software, Inc.).

To observe organogenesis, specimens were fixed in 4% paraformaldehyde in seawater for 45 min and then washed two to three times in 1× PBS. Specimens were stored at 4 °C before they were stained with propidium iodide or Hoechst 33342 and either Alexa-488 phalloidin or BODIPY-FL phallicidin (PH) (Molecular Probes, Inc.). Stained embryos were mounted in VectaShield (Vector Laboratories) or were examined in PBS to avoid distortion of the larval body. Specimens were examined on either a Zeiss 310 LSCM, a BioRad Radiance 2000 LSCM, or an Olympus FluoView FV1000 LSCM, using either a 60× oil 1.4 NA Plan Apo, 40× oil 1.3 NA Plan Fluor, or 20× 0.75 NA Plan Apo objective. Confocal Z-series were projected using ImageJ 1.42. In a few cases (Fig. 5A and 5B), to better reveal cell outlines, autofluorescent yolk was subtracted by computational image processing as follows: because the yolk granules appear in both blue and green channels, these images were multiplied together, then the square root of this product image was computed. The resulting "background" image emphasizes information shared between the two channels, and was therefore scaled to match the yolk fluorescence in each channel and subtracted from the original images.

Specimens for scanning electron microscopy were fixed two ways: (1) with 2.5% glutaraldehyde in Millonig's phosphate buffer for 30 min, followed by two washes in Millonig's phosphate buffer, then post-fixed with 4% osmium tetroxide in Millonig's phosphate buffer for 30 min, followed by two washes in Millonig's phosphate buffer; or (2)

directly fixed in 4% osmium tetroxide in seawater for 30 min, then washed twice with FSW and distilled water over a 24-h period.

Larvae were reared through metamorphosis using standard techniques for polychaetes (Strathmann, 1987). Larvae were kept in 4-l glass culture jars at a density of 1/ml and gently stirred with acrylic plastic paddles. Cultures were cleaned every other day with FSW and fed a mixture of *Rhodomonas lens* and *Isochrysis galbana* (5,000 and 10,000 cells/ml, respectively).

Results

General embryology

Gametes are loose in the coelom in mature males and females and can flow between segments, although they are much more tightly packed in the mid-abdominal segments than in the posterior segments. Spermatozoa either singly or in bundles (*i.e.,* late-stage rosettes with heads packed together and tails radiating outward) and primary oocytes are spawned through paired pores at the posterior end of the animal. Upon contact with seawater, rosettes break apart into individual spermatozoa. Sperm have a small head (4 μm) and long flagellum (30 μm). Newly released eggs, whether spawned naturally or removed from ripe females, had an irregular shape, a pronounced germinal vesicle, a spawning membrane, and a jelly coat (Fig. 1A). Within an hour or two of coming into contact with seawater, eggs became spherical and underwent germinal vesicle breakdown (Fig. 1B). Eggs are colorless, nearly clear, and 70–80 μm in diameter. Removal of the jelly coat does not prevent fertilization or development, but removal of the spawning membrane does. Eggs could be fertilized only after the completion of germinal vesicle breakdown.

Cleavage follows the spiral pattern through the 128-cell stage. The first polar body forms about 1 h post-fertilization at 12 °C, followed by a second after another hour and fusion of the pronuclei (Fig. 1C, D). The first two divisions are meridional and occur at 3 and 4 h post-fertilization, respectively (Fig. 1E–J). Cleavage is dexiotropic and unequal at the 8-cell stage: the animal cells (micromeres) are larger than the vegetal cells (macromeres) (Fig. 1K–N). The spiral nature of embryos is slight and somewhat variable at third cleavage, relative to other spiralian embryos, but becomes more pronounced in later cleavages. Fourth cleavage is meridional and more distinctly spiral (Fig. 1 O–Q). The blastocoel, which first becomes apparent in the 8-cell stage, is very pronounced beginning with the 32-cell stage (Fig. 1R, S), and remains obvious throughout embryogenesis. At the 64-cell stage, the vegetal portion of the blastula thickens, forming a flat plate prior to gastrulation (Fig. 1T).

Gastrulation begins about 8–9 h post-fertilization, after the seventh cleavage or the 128-cell stage. Gastrulation clearly takes place by invagination: vegetal cells constrict at their apical ends as their basal regions extend into the blastocoel (Fig. 2A, B), while retaining neighbor relations, such that approximately the vegetal-most third of the blastula buckles inward. After this initial rearrangement, the vegetal cells resume dividing, and within 4 h the archenteron takes up the majority of the blastocoel (Fig. 2C). The invaginated archenteron retains a narrow but definite lumen. The blastopore remains open throughout gastrulation and is situated initially in the center of the vegetal pole of the embryo (Fig. 2C–H; Supplemental Movie 1, http://www.biolbull.org/supplemental/).

Once the archenteron reaches the animal end of the blastocoel, it folds over to one side (Fig. 2E). Curiously, the polar bodies disappear at about this time. In time-lapse video we observed them to suddenly migrate through the epithelium of the animal pole, and then disappear. Staining with Hoechst revealed the bright, condensed nuclei of the polar bodies; once in the blastocoel, they appear to be engulfed by cells at the tip of the archenteron. If, as seems likely, they remain in place as the archenteron deforms, this phenomenon provides a potentially useful marker for the archenteron tip. Shortly after the archenteron makes contact with the apical pole, a group of cells appears near the base of the archenteron and extends toward the top portion of the archenteron, which is now folded over (Fig. 2F). These cells appear to be the larval mesoderm, which we suspect will form larval muscles such as the dorsal levators, and possibly the larval nephridia. At the opposite side of the archenteron, the surface of the embryo protrudes just below the mesodermal pockets (Fig. 2G). This area forms the chaetal sac and chaetae of the mitraria larva. At 22 h post-fertilization, one of two pairs of dorsal levator muscles connecting the chaetal sac to the apical epidermis has formed, confirming the location of the chaetal sac (Fig. 2H).

Our conclusion, based on the location of the chaetal sac, the folding of the archenteron, and the relative locations of the stomodeum, anus, and chaetal sac in the earliest swimming larval stage, is that the blastopore becomes the opening immediately adjacent to the chaetal sac in the larva and thus forms the anus. The continuous presence of a blastopore in time-lapse films (Fig. 2) and at all stages of gastrulation that we have analyzed by fixation (Fig. 3) support this conclusion. Our time-lapse videos do not unambiguously show the formation of a mouth and esophagus, likely because the larvae begin to swim just as this process commences. At 24 h, examination of fixed larvae by confocal microscopy showed that the mouth and anus of the larva are both present and open (see Larval Development below). The mouth and esophagus may form as either an extension of the blastopore or as a secondary invagination, connecting it to the archenteron with the anus between it and the chaetal sac. Because the archenteron appears to fold over to meet another group of cells arranged in a funnel

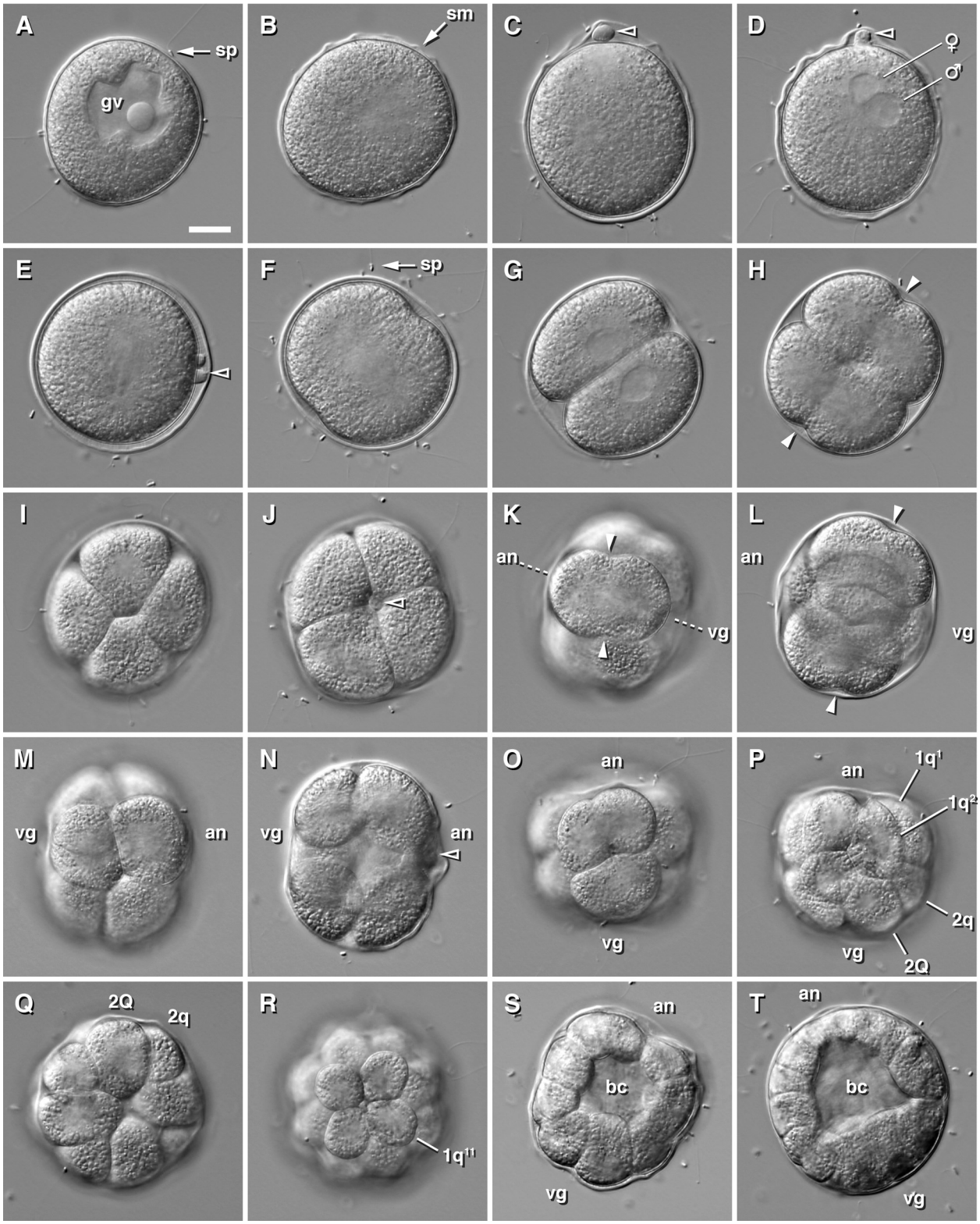

Figure 1. Early embryonic development of *Owenia collaris*. (A) Newly spawned primary oocyte with germinal vesicle (gv) and sperm (sp) trapped in the jelly coat (the jelly coat is invisible). (B) Newly fertilized zygote with spawning membrane (sm). (C) Fertilized zygote after release of first polar body (open arrowhead). (D) Fertilized zygote after release of second polar body; male and female pronuclei are about to fuse. (E) Metaphase of first cleavage. (F) Telophase of first cleavage. (G) 2-cell stage. (H) Second cleavage (filled

shape that opens just behind the primary ciliated band (see below), we suggest that the mouth forms as a secondary invagination. However, cell lineage studies will be required to evaluate this hypothesis.

Ciliated band formation

Cilia form relatively late in embryos of *O. collaris*, and embryos lack obvious signs of cleavage arrest in the cells that would be the primary trochoblasts in a canonical spiralian (the granddaughters of the $1q^2$ cells, which themselves are the vegetal daughters of the first quartet of micromeres formed at third cleavage). Time-lapse video shows that descendants of the $1q^2$ cells continue to divide well beyond the typical point of cleavage arrest (Fig. 2A–H; Supplemental Movie 1, http://www.biolbull.org/supplemental/). The sizes of nuclei and cells continue to decrease during gastrulation throughout the ectoderm, including the zone occupied by $1q^2$ descendants. Nucleus diameter decreased from 5 μm to 3 μm to the point that they cannot easily be distinguished in live embryos (Fig. 2A, C, E, respectively). The diameter of these cells along the animal-vegetal axis decreased from 11 to 7 to 5 μm at the same timepoints.

Typical annelid embryos initiate ciliogenesis at the 64-to 128-cell stage, which in *O. collaris* corresponds to 8 h post-fertilization, but cilia do not appear in *O. collaris* until 19 h after fertilization at 12 °C (Fig. 2G). By this point, gastrulation has taken place and the archenteron is well developed. When cilia first form, each is isolated from the others, and at no point are compound cilia from a few large cells observed (Fig. 2I), as one would expect to see during the formation of the prototroch in a trochophore. The primary ciliated band (analogous to the prototroch) is formed by a double row of simple cilia uniformly arranged around the embryo (Fig. 2I). Mitotic figures are evident among the small cells within the primary ciliated band (Fig. 3) long after the point at which, in a canonical trochophore, one would expect to find a distinct band of very large, cleavage-arrested cells. The region of ciliated band formation is initially spread out around the equator of the embryo (Fig. 3A–C), but becomes organized into the double row of ciliated cells around 20 h post-fertilization (Fig. 3D). Cells in the primary ciliated band continue to divide *in situ* within the band at least until just prior to hatching (Fig. 3E, F), and probably throughout larval life. In embryos of *O. collaris*, bilateral symmetry first becomes evident during development of the ciliated band, when the pattern of cell divisions reveals an approximate right-left axis of symmetry passing through the digestive system. This coincides with the bending of the archenteron and the emergence of mesodermal cells within the blastocoel.

Larval development

Cultured larvae require about 4 weeks at 12 °C and 3 weeks at 16 °C to develop a juvenile rudiment and reach competence to metamorphose. At 24 h post-fertilization, larvae begin to swim off the bottom of culture dishes. Larvae do not hatch out of the spawning membrane, but rather the cilia of the apical tuft and primary ciliated band grow through it (Fig. 2I). Further growth of the epidermis and gut separate the mouth and the anus, but the digestive system remains strongly horseshoe-shaped. Because of the strong curve of the digestive tract, the ventral surface at this point consists of only the tissue between the mouth and anus. The ventral surface grows minimally by comparison to the dorsal surface, or episphere, of the larva. The episphere of a young larva is relatively opaque with many cells closely packed together, but soon the episphere expands as the cells of the epidermis become thinner and therefore less dense, and the episphere becomes nearly transparent (Fig. 4A–E).

At the time that larvae begin swimming, both the mouth and anus appear to be open (Fig. 5A), although the persistence of the spawning membrane may mean they are not yet open to the environment. The mouth opens to a funnel-shaped group of cells (mentioned previously), which form the esophagus and connect to the larval mid-gut. Within 2 to 3 days the mitraria has formed its first two to three pairs of chaetae (Figs. 4A, 5B), and both the chaetal sac and esophagus have become highly muscular (Fig. 5C). The chaetal sac contains two chaetal glands connected by a system of interwoven muscles that surround the glands in a figure-eight pattern. The dorsal levators increase in size in the next few days, becoming more distinct (Fig. 5D). These muscles connect the chaetal sac to the apical organ, which at this stage contains a pair of red larval eyes. The chaetal sac is also connected to the esophagus by muscles running along the ventral surface of the larva (Fig. 5C).

arrowheads indicate nascent furrow). (I) 4-cell vegetal pole with cross furrow. (J) 4-cell animal pole; open arrowhead indicates polar body. (K and L) Side view of third cleavage showing slight tilt of the division axis (arrowheads) relative to the animal-vegetal axis (dashed line), and slight inequality of division along the animal-vegetal (an-vg) axis. (M and N) Side view of 8-cell stage showing spiral nature of the previous division, and relative sizes of micro-and macromeres. (O) Side view of fourth cleavage. (P) Side view of 16-cell stage with the four cells of one quadrant labeled. (Q) 16-cell vegetal pole. (R) 32-cell animal pole with definite spiral arrangement. (S) Side view of 32-cell stage with open blastocoel (bc). (T) Side view of 64-cell stage. Scale bar: 20 μm.

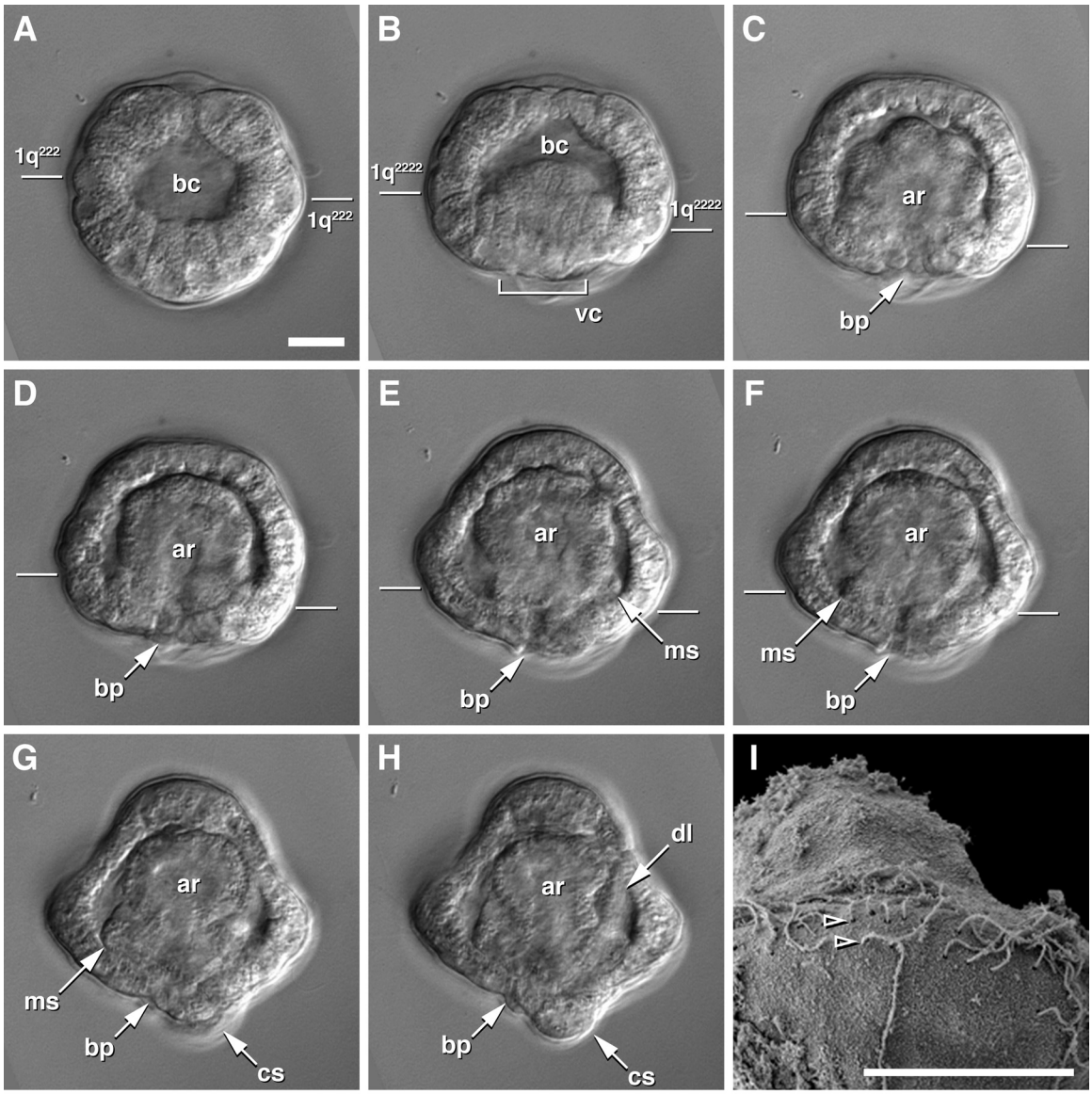

Figure 2. "Trochoblast" division and gastrulation in *Owenia collaris*. Horizontal lines indicate location of $1q^2$ descendants (primary trochoblasts in typical spiralian embryos) and area of cilia development in E and F. Reduction of nucleus and cell diameters to the point that individual cells are indistinguishable indicates continued division of $1q^2$ descendants (see Supplemental Movie 1, http://www.biolbull.org/supplemental/). (A) 6-h embryo, coeloblastula with open blastocoel (bc) prior to gastrulation and after the second division of the $1q^2$ cells. (B) 8-h embryo, initiation of gastrulation as vegetal cells (vc) invade the blastocoel. (C) 12-h embryo, initial invagination reaches the blastocoel roof; the archenteron (ar) has a lumen that opens to the blastopore (bp) at the vegetal pole. (D) 13-h embryo, archenteron nearly fills the blastocoel. (E) 16-h embryo, archenteron begins to fold toward the future larval anterior (left) after making contact with the roof of the blastocoel. The blastopore remains open and mesoderm (ms) cells appear within the blastocoel. The equatorial margin begins to protrude where the primary ciliated band will form. (F) 17-h embryo, appearance of mesodermal cells between the archenteron and the ectoderm (ms). The blastopore remains open. (G) 20-h embryo, the chaetal sac (cs) protrudes, and mesodermal cells form two distinct masses. (H) 22-h embryo, development of dorsal levators (dl) connecting chaetal sac to apical pole. (I) scanning electron micrograph of 22-h embryo, double row of cilia (open arrowhead) forming the primary ciliated band. Scale bars: 20 μm.

Within days of hatching, the ciliary band, which is predominantly bright orange when viewed with transmitted light, contains hundreds of cells (Figs. 4B, 5D). The primary ciliated band begins as a simple ring, but soon folds dorsally at the anterior and posterior ends of the larva (Figs. 4B, 5E). As the mitraria grows, folds also appear on either side of the

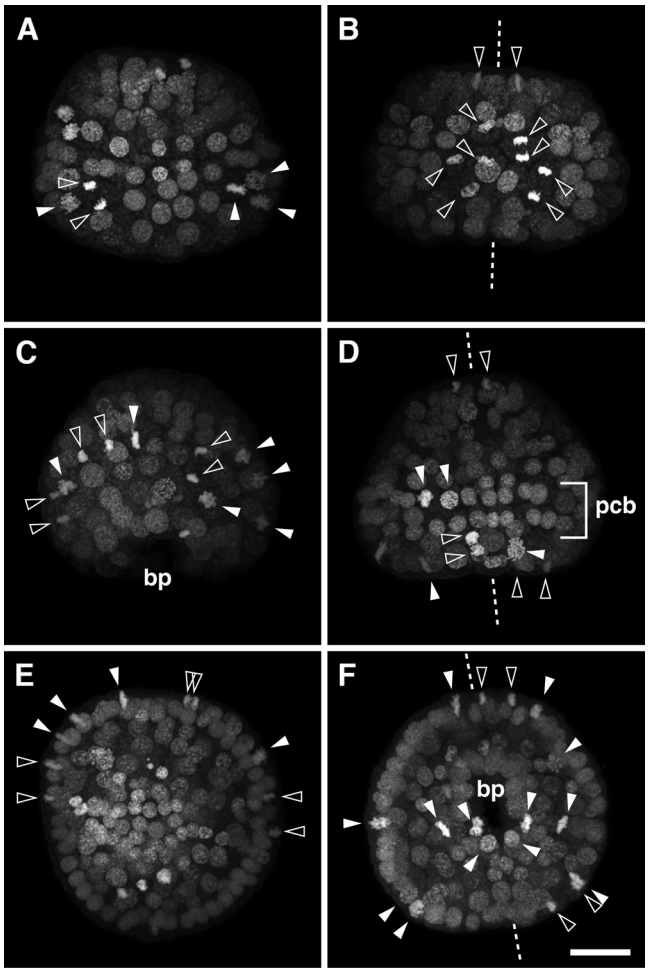

Figure 3. Mitotic cells during formation of the primary ciliated band in *Owenia collaris*. Hoechst-stained embryos at 17-h (A, B), 20-h (C, D), and 22-h (E, F) post-fertilization; projected serial confocal sections. The animal pole is up in panels A–D. In all panels, outlined arrows denote pairs of sister chromatids or recently divided cells, and filled arrowheads denote cells just prior to division, with condensed or aligned chromosomes. (A) Slightly oblique lateral view of divisions along the equator in the region of the developing primary ciliated band of the embryo and at the animal pole. (B) Lateral view showing that an approximate axis of bilateral symmetry (dashed line) is already evident on the basis of the location of dividing cells in the embryo. (C) Slightly oblique lateral view. At this stage, cell divisions in the equatorial region occur both along the animal-vegetal axis and along the equatorial axis of the embryo. bp = blastopore. (D) Lateral view. Cells in the region of the primary ciliated band (pcb) are aligned in a double row of cells. (E) Animal/dorsal view of cells dividing in place within the region of the primary ciliated band. In contrast to panel C, all cell divisions within the band occur along the equator. (F) Vegetal/ventral view of cell division within the ciliated band and on either side of the axis of bilateral symmetry. Scale bar: 20 μm.

larva, forming lappets (Figs. 4C, 5E). A secondary ciliated band (analogous to the metatroch) and food groove complete the ciliated-band system (Figs. 4E, 5E, G), but their origins have not been identified. Algal cells are often entrained into the broad food groove between the primary and secondary ciliated bands from the posterior end of the larva and travel along these folds to the anteriorly located mouth.

The juvenile rudiment in *O. collaris* first appears as an epidermal invagination on the larval ventral surface between the mouth and anus 2 weeks post-fertilization at 12 °C (Figs. 4C–E, 5E, F). This invagination grows to occupy most of the hyposphere below the curve formed by the esophagus, mid-gut, and hindgut (Fig. 4D, E). Within days, this fold grows up along the anterior portion of the hindgut and forms a pocket that fills the space ventral to the digestive system, while at the same time the ciliated band has formed all four of its lappets, or downward folds (Fig. 4D, E). At about 18–21 days, small sacs form on the inner, blastocoelic surface of the rudiment (Fig. 6A–C; Supplemental Movie 2, http://www.biolbull.org/supplemental/). These sacs (thread glands in Wilson, 1932) are destined to become the first nephridia in the adult worm, derived from the ventral epidermis of the larva. During this phase, chaetae and rows of uncini develop within each segment (Fig. 6C). The basal portions of the juvenile rudiment are always continuous with the ventral epidermis of the larva, and the pocket remains open to the outside.

As the pocket becomes deeper and wider, it wraps around the hindgut (Fig. 6D–F; Supplemental Movie 3, http://www.biolbull.org/supplemental/). Somehow the margins of the pocket fuse around the posterior side of the hindgut, such that the fully developed juvenile rudiment envelops the hindgut in the manner of a sock that is partly rolled inside-out. The portion of the rudiment that will form the posterior—the foot of the sock—is configured around the gut as it will be after metamorphosis, whereas the anterior half—the leg of the sock—is peeled back (see Metamorphosis below; the toe of the sock, in this metaphor, corresponds to the extreme posterior of the juvenile worm). By the time the rudiment fully encircles the hindgut, not only are the nephridia, chaetae, and uncini present, but also the segmental body wall musculature, chaetal musculature, and future coelomic lining have formed (Fig. 6D–F). The coelomic lining develops as a thin layer around the rudiment and forms a septum between the first two pairs of nephridial sacs and the rest of the nephridial sacs (Fig. 6D). The juvenile buccal organ also forms ventral to the larval stomodeum (Fig. 6C, F). At the time of metamorphosis, these internal juvenile structures elongate and straighten as the adult ectoderm and mesoderm—the sock—unrolls around the digestive tract, but all retain their positions relative to one another (Fig. 6G–I).

Metamorphosis

Prior to metamorphosis, larvae typically sink to the bottom of culture jars and the trunk segments begin to protrude from the larval hyposphere (Fig. 7A). Once the trunk segments protrude, the larval episphere begins to shrink and

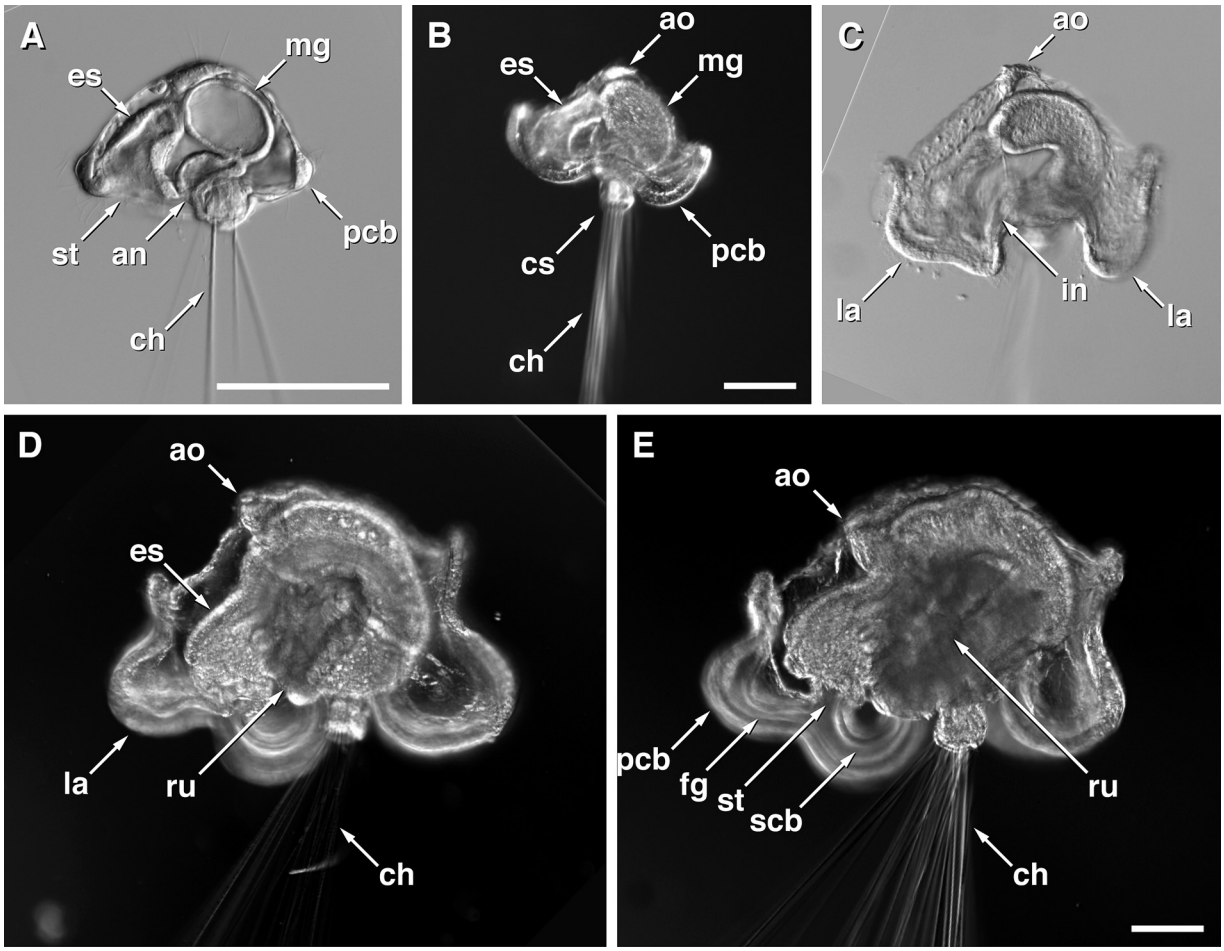

Figure 4. Development of the mitraria larva in *Owenia collaris*. (A) 48-h larva, side view, with first two pairs of larval chaetae (ch) and fully formed digestive system from stomodeum (st) to anus (an), with esophagus (es), mid-gut (mg), and hindgut surrounded by the primary ciliated band (pcb). (B) 7-day larva, darkfield side view, with ciliated band system folding at anterior and posterior ends and developing apical organ (ao) and chaetal sac (cs) with 5–6 pairs of chaetae. (C) 14-day larva, side view, with ciliated band system folded to form lappets (la). The juvenile rudiment invagination (in) is present but is partially obscured behind the ciliated band. (D) 24-day larva, darkfield side view of advanced mitraria with fully developed ciliated band system and developing juvenile rudiment (ru). (E) 24-day larva, darkfield side view, focused on primary and secondary ciliated bands (scb) and food groove (fg) leading to stomodeum. Scale bars: 100 μm.

retract, as if deflating around the gut (Fig. 7B, C). The cilia of the ciliated bands still beat and propel the animal, but the band folds in on itself and slowly disintegrates (Fig. 7B, C). At the same time, the trunk begins to straighten out: as the sock unrolls, the digestive tract is pulled down and enclosed, with the anterior nephridia and juvenile musculature adopting their appropriate positions (Fig. 7C; summarized diagrammatically in Fig. 8).

Although Wilson described the juvenile worm of *O. fusiformis* consuming the larval episphere, there is no compelling evidence that this occurs in *O. collaris*. The ciliated band remains distinctly bright orange, but this color is absent from the gut after the ciliated band has disappeared, and in most cases, the gut is empty after metamorphosis except for small clumps of consumed algae (Fig. 7D). The larval episphere simply shrinks and becomes incorporated into the juvenile worm's head. In Figure 7D–F, one can see the remainder of the larval episphere shrinking onto the dorsal side of the worm while the mouth of the juvenile remains unencumbered by this tissue on the ventral surface. The episphere continues to recede, and the dorsal levators contract and pull the apical organ toward the esophagus until it becomes attached to the juvenile body (Fig. 7G). One of the final larval features to be lost is the chaetal sac (Fig. 7E, G). The chaetae are shed once the episphere has collapsed, and the sac itself is resorbed into the anterior collar of the worm.

The process of metamorphosis in *O. collaris* can be summarized as follows. Initially, nephridial pair 4 resides roughly at the ankle of the sock, where it is folded over, and

the larval esophagus and mid-gut reside entirely outside the sock; nephridial pairs 1–4 hang into the blastocoelic space from the unrolled leg, whereas pairs 5–7 reside inside the foot of the sock along with the larval hindgut (Fig. 8D, D′). The leg of the sock turns right-side-out during metamorphosis, after which all the nephridial pairs and the entire digestive system are now inside the sock. The larval ciliated bands disappear; the larval epidermis is resorbed or incorporated into the collar of the juvenile worm, and the apical organ caps the head.

Juvenile worm morphology

After metamorphosis, juveniles are about 815 μm in length and 125 μm diameter, averaged from 20 juveniles obtained in a single culture (Table 1). The young worm is equipped with a head (prostomium and peristomium), one thoracic segment bearing two sets of chaetae, six or seven segments each bearing a single pair of chaetae and one pair of tori (rows of uncini located in the middle of each segment), and a pygidium (Figs. 7G–I, 9A). The chaetae and uncini, which were present before metamorphosis, now can be seen clearly along the trunk segments. The juvenile worm retains the larval eyes as part of the fused pro- and peristomia, although they are generally lost in the adult (Figs. 7I, 9B). Internally, the thoracic segment typically inherits the first two pairs of nephridia, matching the two pairs of juvenile chaetae. This segment is separated from the subsequent abdominal segments by a thin septum that was present in the larva (Fig. 6D, H). The first chaetigerous segment inherits the third pair and the longest pair of nephridia (4), which probably become fused, as adults have only one pair of nephridia in each abdominal segment. One pair of nephridia resides in each of the next three chaetigerous segments (Fig. 9A), although these appear to be bilobed at metamorphosis (Fig. 6H). The external demarcation of segments by chaetae and tori is not exactly mirrored internally by the location of the nephridia. However, the absence of segmental septa in the abdominal region of the worm allows the movement of nephridia between segments. The position of the septum between thoracic and first abdominal segments suggests, in any case, that the tori do not correspond to the edges of the segments, but rather lie slightly anterior to the middle of each segment.

Soon after metamorphosis, the juvenile begins to gather materials for its initial tube and often sticks to surfaces with its anterior end (Fig. 9A). The initial tube is generally made of clear mucus and small particles such as algal cells and bacterial film, but can also contain much larger items such as threads, larval chaetae, and the tubes of other worms (Fig. 9B). Within the first week, juveniles also develop a pronounced sphincter at the opening to the mid-gut, and incomplete coelomic compartments (Fig. 9C). When offered sediment, young worms commonly use the smallest grains to add to their tubes or will shed the initial tube and replace it with one anchored into the sediment (Fig. 9D). At first, juveniles of *O. collaris* lack tentacles, but these soon form in pairs of buds (Fig. 9E). Within 2 weeks, juveniles grow three pairs of unbranched, prostomial tentacles. Like the adults, juveniles are surface deposit feeders, consuming small grains of sediment as well as whatever is attached to them (Fig. 9E). When held in the laboratory, juveniles grow to a length of about 1300 μm by 24 days after metamorphosis (Table 1).

Discussion

Although embryonic development in many annelid taxa conforms well to long-established protostome stereotypes, many species display modifications of the spiralian cleavage pattern, diverse modes of gastrulation, and of course varied larval forms. *Owenia collaris* exhibits shared features of development for annelids and protostomes, but also modifications to the stereotypical patterns. At the 8-cell stage, animal cells (micromeres) are larger than the vegetal macromeres, similar to all nemerteans but unlike most annelids (Shankland and Savage, 1997). This may represent an adaptation of the cleavage program to provide sufficient cells to establish the disproportionately large episphere of the mitraria, and therefore may also suggest that this embryo retains some cell lineage constraints from the spiralian stereotype.

Owenia collaris embryos undergo holoblastic spiral cleavage to form a coeloblastula, which, although exceptionally hollow (again like some nemerteans), conforms to the ancestral pattern for annelids (Okada, 1970). Past this point, several key features of *Owenia*'s development diverge from the protostome stereotype. The stomodeum does not appear to be derived from either the blastopore or the area in which the blastopore forms. The mouth may form as a secondary opening, while the anus alone develops from the blastopore, which appears to remain a small, circular opening throughout gastrulation. We see no sign that the blastopore elongates to form both mouth and anus through lateral compression (Nielsen, 2001). In other words, we see no evidence for literal protostomy in *Owenia*; this embryo appears to be, in the literal sense, deuterostomous. Although rare, this is not unheard of in annelids or other protostome groups. In the polychaete *Eunice kobiensis,* the anus also forms in the region in which the archenteron opens, and the stomodeum forms as a separate, secondary invagination (Akesson, 1967). However, in the case of *E. kobiensis*, the blastopore closes after gastrulation and later in development the anus opens in the same position. But in the gastropod *Viviparus*, as in *Owenia*, the stomodeum forms as a secondary invagination and the anus is derived from the blastopore (Dautert, 1929; Fernando, 1931). Cell lineage studies will be required to confirm the fate of the blastopore and origin

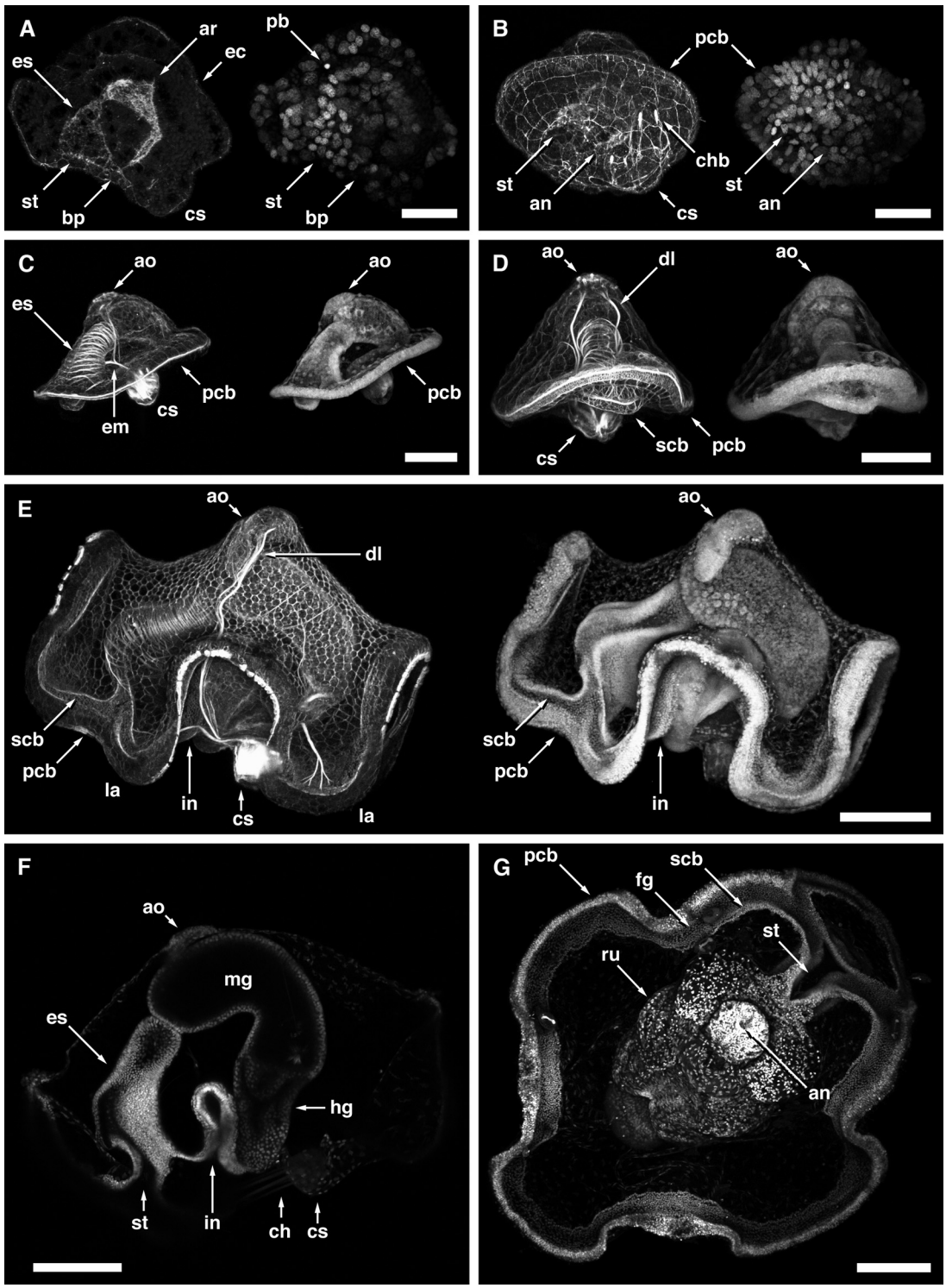

Figure 5. Development of the mitraria larva in *Owenia collaris*. A and B are stained with phalloidin and Hoechst; C–E with phalloidin and propidium iodide; F and G with Hoechst alone. (A) A 24-h-old newly swimming larva viewed from the side with two cells layers: the larval ectoderm (ec) and endoderm formed by two pockets of tissue, one composed of the archenteron (ar) and blastopore (bp) anterior to the chaetal sac (cs) and the other composed of the stomodeum (st) and esophagus (es); one of the polar bodies (pb) can be seen between the two tissue layers; projection of 9 confocal sections, 4-μm apart, background-subtracted to suppress autofluorescent yolk. Scale bar: 25 μm. (B) 24-h newly swimming larva viewed from the larval hyposphere with cells of the primary ciliated band (pcb) organized into two rows, open stomodeum and anus

of the stomodeum in *O. collaris*. To date we have found this impossible in this species due to the difficulty of either removing or piercing the spawning membrane.

In *O. collaris* the fate of the primary trochoblast ($1q^2$) lineage also diverges from typical polychaetes. The derivatives of this lineage, which would generally undergo cleavage arrest and become multiciliated to form the prototroch in canonical trochophores, remain mitotically active and develop a single cilium each in the *Owenia* hatchling. The primary ciliated band in *O. collaris* develops through continued proliferation of cells that, although they may be derivatives of the trochoblast lineage, form cilia much later in development than spiralian embryos of similar size (Rattenbury and Berg, 1954; Okada, 1970; Smith, 1981; Strathmann, 1987). The cells that make up the primary ciliated band are also much smaller than those of other protostomes, as is expected if they undergo continued division. Estimates of ciliated band cell diameters for *O. collaris* after ciliation are in the range of 4–5 μm, whereas those for the nemertean *Carinoma tremaphoros*, the polychaetes *Nereis limbata* and *Polygordius* sp., and the limpet *Patella vulgata* are 25–50, 11–22, 15, and 30 μm, respectively (Maslakova *et al.,* 2004; Costello, 1945; Woltereck, 1902; Damen and Dictus, 1994). Although composed of smaller cells, the primary ciliated band in early larvae of *O. collaris* covers about the same fraction of the total surface area of the larva when compared with early trochophores of other polychaetes (14% as compared to 11%–38% for other polychaetes; Costello, 1945; Anderson, 1959; Akesson, 1967).

Adult *Owenia* spp. also possess deuterostome-like epidermis and nephridia, a conclusion based on the fact that monociliated cells dominate both tissues (Gardiner, 1978; Smith *et al.,* 1987). Monociliated cells are also found in larval and adult *Magelona mirabilis* (Bartolomaeus, 1995). The closest relatives of *Owenia* spp. and *M. mirabilis* within the polychaetes, however, possess multiciliated cells (Gardiner, 1979; Bartolomaeus, 1995; Rouse and Fauchald, 1997). Bartolomaeus (1995) therefore concluded that monociliarity in both *Owenia* and *Magelona* is secondarily derived, and he suggested that multiciliarity is suppressed in an early stage of ciliogenesis.

It is phylogenetically implausible that the deuterostome-like traits we describe in *Owenia* could reflect retention of or simple reversion to the plesiomorphic condition of the *Urbilateria*. Recent morphological and molecular phylogenies of annelids place the Oweniidae well within the Canalipalpata, as a member of either the Sabellida clade or a clade containing the Polygordiidae (Rouse and Fauchald, 1997, 1998; Rouse, 1999). The alternative is that, as Bartolomaeus (1995) concluded for monociliation, the deuterostome-like traits of *Owenia* embryogenesis—including gastrulation by invagination into a hollow blastocoel, literal deuterostomy, and formation of ciliated bands from proliferating cells—are secondarily derived characteristics that superficially resemble equivalent characteristics of true (that is, phylogenetic) deuterostomes by convergence. Convergent evolution of traits like literal deuterostomy in *O. collaris* undermines classical arguments that placed the lophophorates in the deuterostome super-clade on the basis of these or similar embryological characteristics (Zimmer, 1964). Recent phylogenetic analyses using molecular sequence data concur that lophophorates belong within the lophotrochozoan clade (Aguinaldo *et al.,* 1997; Aguinaldo and Lake, 1998; Peterson and Eernisse, 2001; Bourlat *et al.*, 2008), and it seems to us that the case of *Owenia* obviates any apparent conundrum posed by deuterostome-like traits of lophophorate embryos.

Our description of rudiment development and metamorphosis in *Owenia collaris* is largely concordant with Wilson's classic study of *O. fusiformis* (Wilson, 1932). However, comparisons between *O. collaris* and *O. fusiformis* reveal minor differences in development that can be used to distinguish the two species as larvae and juveniles (Wilson, 1932). *Owenia collaris* and *O. fusiformis* differ in size

(an), and chaetal sac with chaetoblasts (chb) forming first two pairs of larval chaetae; projection of 85 confocal sections, 0.4-μm apart. Background-subtracted to suppress autofluorescent yolk. Scale bar: 25 μm. (C) 3-day larva viewed from the side, revealing musculature of esophagus, chaetal sac, primary ciliated band, and the connection between esophagus and chaetal sac (em), and that cell nuclei are densest in the primary ciliated band and apical organ (ao); projection of 34 confocal sections, 3-μm apart. Scale bar: 50 μm. (D) 4-day larva, anterior view, illustrating musculature connecting the apical organ to chaetal sac around the digestive system or dorsal levators (dl), and cell outlines and muscles running through the primary ciliated band and secondary ciliated band (scb); cell nuclei are highly concentrated within the ciliated bands; projection of 123 confocal sections, 0.8-μm apart. Scale bar: 50 μm. (E) 17-day larva; the juvenile rudiment invagination (in) has expanded to fill the hyposphere below the digestive system, and larval musculature is fully developed with dorsal levators (dl) and chaetal sac, and fully formed ciliated band system with primary ciliated band, secondary ciliated band, and lappets (la); projection of 52 confocal sections, 3-μm apart. Scale bar: 100 μm. (F) 17-day larva; cross-section of early rudiment invagination below the larval digestive system complete with esophagus, mid-gut (mg), and hindgut (hg); projection of 11 confocal sections, 1-μm apart. Scale bar: 100 μm. (G) Ventral view of advanced mitraria with fully developed rudiment (ru), showing the primary and secondary ciliated bands, with food groove (fg) in between, splitting in front of the stomodeum; projection of 148 confocal sections, 1.2-μm apart. Scale bar: 100 μm.

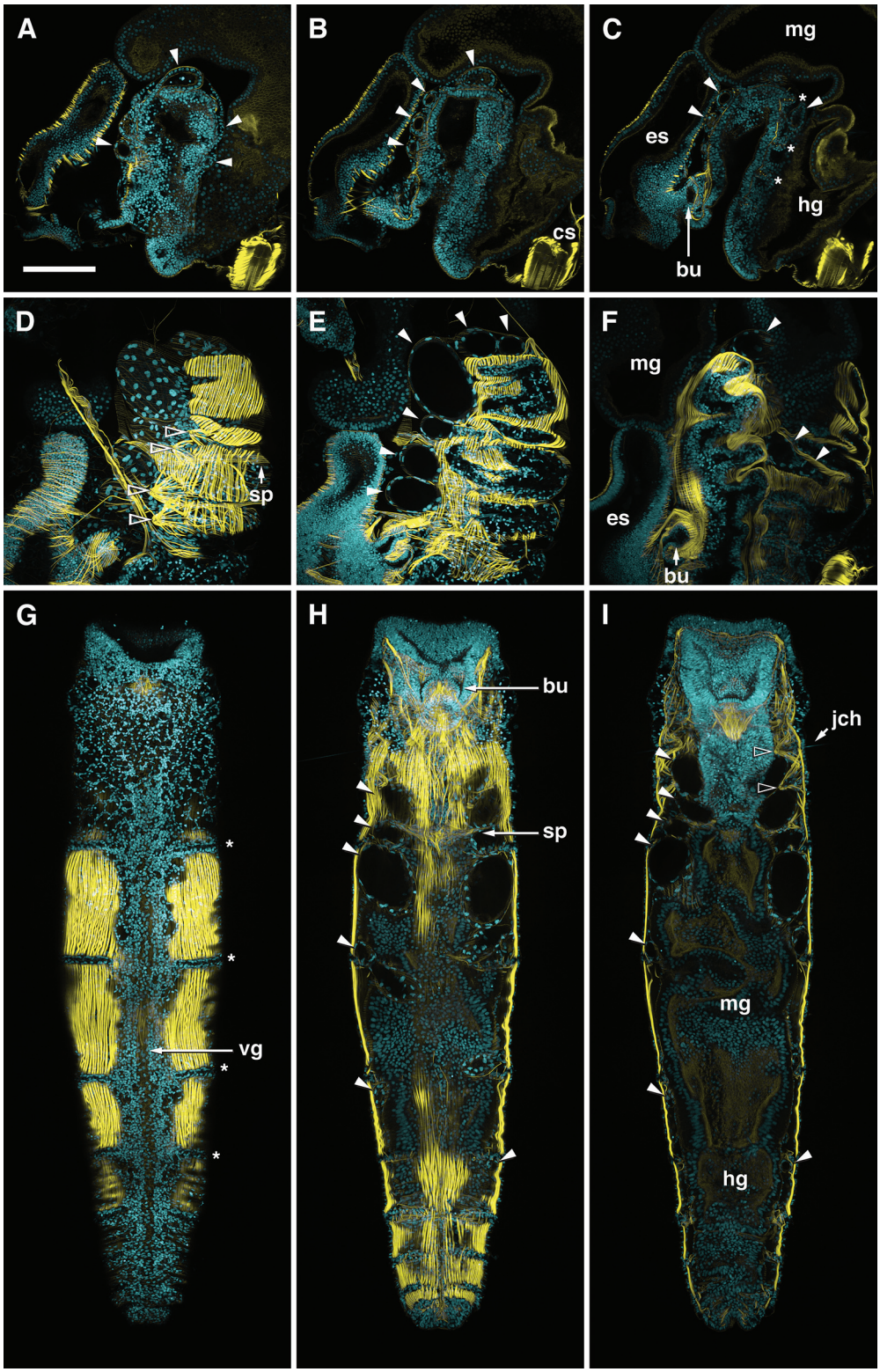

Figure 6. Internal anatomy of juvenile structures of *Owenia collaris*. All panels show phalloidin in yellow and Hoechst in cyan. Scale bar in A is 80 μm and applies to all. (A–C) Intermediate-staged mitraria with juvenile rudiment invagination below esophagus (es) and above chaetal sac (cs), not yet enclosing the hindgut (hg) or mid-gut (mg) but filling the space beneath the digestive tract. The juvenile buccal organ (bu) has formed below the larval stomodeum. Solid arrows denote developing nephridial sacs and asterisks (*) denote the location of tori or rows of uncini, which at this stage stain brightly with phalloidin. Each panel is a projection of five consecutive 0.6-μm confocal

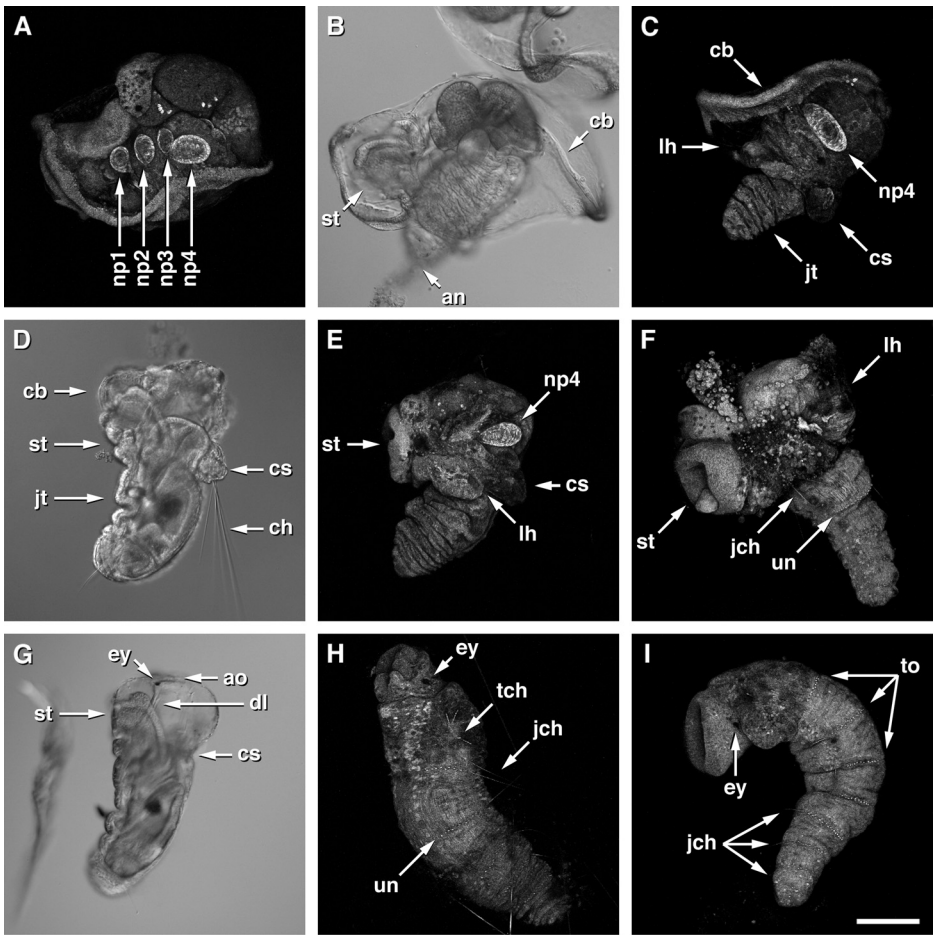

Figure 7. Metamorphosis of *Owenia collaris*. A, C, E, F, H, and I are projections of confocal Z-series, stained with propidium iodide. (A) 27-day, fully developed rudiment with first four sets of nephridial sacs (np) visible. (B–G) 30-day. (B) Initiation of metamorphosis by extension of rudiment just below stomodeum (st) and above anus (an), and breakdown of ciliated bands (cb). (C) Extension of juvenile trunk (jt) past the chaetal sac (cs) and larval hyposphere (lh), which has yet to unfold past the fourth pair of adult nephridia (np4). (D) Retraction of larval episphere onto dorsal surface of juvenile and onset of resorption of the chaetal sac with larval chaetae (ch) still attached into dorsal surface. (E) Resorption of chaetal sacs into dorsal surface, with anterior portion of juvenile digestive system with nephridial pairs 1–4 still above fold of the larval hyposphere. (F) Elongated trunk with juvenile chaetae (jch) and uncini (un) demarcating segments. (G) Retraction of dorsal levators (dl) pulls the apical organ (ao) with eyespots (ey) down to fuse with the trunk; the stomodeum remains unencumbered by the degenerating larval episphere. (H) Juvenile 3 h after completion of metamorphosis; larval eye is retained and the thoracic segment has two sets of chaetae (tch), whereas posterior segments have single pairs of chaetae (jch) and rows of uncini (un). (I) Side view of 1-day-old juvenile with rows of uncini or tori (to) denoting the seven abdominal segments. Scale bar: 100 μm.

throughout development, with the former smaller than the latter at each stage (Table 1). During metamorphosis the overall series of events is the same between species, but *Owenia collaris* resorbs its larval tissues rather than casting them off or consuming them. *Owenia collaris* has fewer chaetigerous segments at metamorphosis than *O. fusiformis*.

sections. (D–F) late-stage mitraria with fully formed juvenile rudiment surrounding the larval mid-gut (mg) and hindgut (hg) with nephridial pairs, juvenile chaetal muscles (outlined arrows), and juvenile buccal organ (bu). The juvenile septum (sp) between the thoracic segment and first abdominal segment is fully formed at this stage. Each panel is a projection of 10 consecutive 0.6-μm confocal sections. (G–I) Metamorphosed juvenile viewed from the ventral side including the ventral groove (vg) with segmentation denoted by rows of uncini, juvenile chaetae (jch), and nephridial sacs. Each panel is a projection of five consecutive 0.6-μm confocal sections.

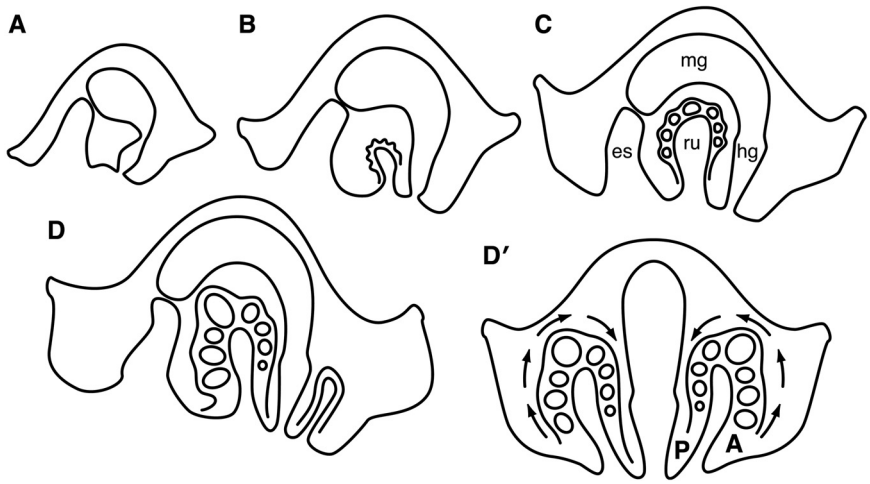

Figure 8. Diagrammatic summary of juvenile rudiment development and organization before metamorphosis in *Owenia collaris*. (A) Sagittal section before appearance of the invagination that will form the juvenile rudiment. (B) Sagittal section; the rudiment expands as a pocket between the mouth and anus. (C) Parasagittal section; expanded rudiment (ru), not yet enclosing the hindgut (hg) but showing typical position of the nephridial sacs (circles); esophagus (es) and mid-gut (mg) would be contiguous at stages represented by B–D, although the connection would only be evident in a true sagittal section. (D and D′) Schematized parasagittal and transverse views just prior to metamorphosis; the "true" axis of the nephridial organs would be diagonal between sagittal and transverse, and the point of this schematic diagram is to show the arrangement of the anterior-posterior axis of the juvenile with respect to the larval body. Arrows in D′ indicate the direction of motion during metamorphosis as the juvenile "sock" unrolls to enclose the gut.

The difference in number of segments continues once tentacles form, probably due to the smaller size of *O. collaris*. This is also reflected in the relative size and number of segments in adults of these two species (Blake, 2000; Koh and Bhaud, 2003). The juvenile trunk of *Owenia* is similar in general structure to the trunk segments of other annelids, with the major difference being that the anterior segments are inverted during the larval stage and all segments are internal prior to metamorphosis.

Table 1

Characteristics of developmental stages in Owenia collaris *and* O. fusiformis

Characteristic	*O. collaris*	*O. fusiformis**
Egg diameter	70 μm	90-120 μm
Larval dorso-ventral diameter at rudiment formation	470 μm	500 μm
Larval dorso-ventral diameter at metamorphosis	475 μm	560 μm
# Nephridia at metamorphosis	7	7
# Fused thoracic segments	2	2
# Chaetigerous segments	6-7	11
Juvenile length at metamorphosis	815 μm	870 μm
Juveniles length at 3-4 weeks	1300 μm	2560 μm

* *Owenia fusiformis* values from Wilson (1932).

Comparing the development of *Owenia* to Woltereck's (1902) classic study of *Polygordius* endolarva development, we also note differences and similarities. These larval forms have in common the presence of an inflated blastocoel. Woltereck (1902) clearly figures multiciliated cells in *Polygordius*' prototroch (plate 5, figures 1 and 4), unlike *Owenia* (Emlet and Strathmann, 1994). While the *Polygordius* endolarval rudiment is folded, accordian-style (Woltereck, 1902, plate 7), at no stage does the rudiment invert the anterior portion; at every stage in *Owenia*, the anterior portion is folded over. Furthermore, although Woltereck (1902) does not illustrate the very earliest stages of rudiment formation in *Polygordius*, it appears to be a circumferential invagination (plate 9, figure 1) such that the dorsal portion of the rudiment forms from the dorsal hyposphere and the ventral portion from the ventral hyposphere; in contrast, in *Owenia* the entire rudiment forms from the "ventral" portion of the hyposphere lying between the mouth and anus, and only encircles the digestive tract after extensive growth and development of rudimentary organs. As with *O. fusiformis*, the prototroch and epi- and hypospheres are cast off to be consumed by *Polygordius*; we have not observed this in *O. collaris*. In all three species, the head fuses with the trunk. Prior to metamorphosis, both oweniids form a buccal organ that is fused with the trunk

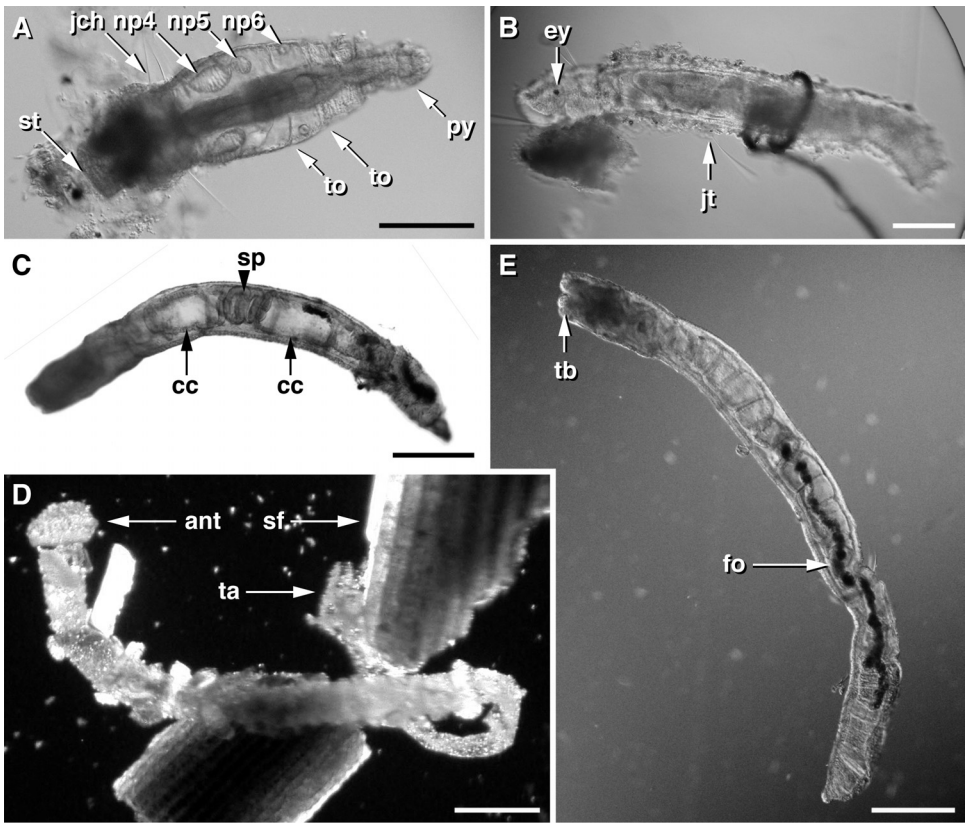

Figure 9. Post-metamorphic development of juvenile *Owenia collaris*. (A) Ventral view of 3-day-old juvenile beginning to gather particles together for initial tube with mucus at anterior end; gut has elongated through the worm, beginning at the stomodeum (st) and terminating in the pygidium (py); juvenile chaetae (jch) and tori (to) are present on each segment, and nephridia (np) can still be seen through the translucent body wall. (B) 5-day-old juvenile with complete juvenile mucus tube (jt) and larval eye (ey) still present. (C) 1-week-old juvenile showing growth of trunk, coelomic compartments (cc), and sphincter (sp) at the entrance to the mid-gut. (D) 2-week-old juvenile with complete sediment tube anchored to a fragment of an urchin spine (sf) at the posterior end (ta) and unattached anterior end (ant). Scale bars: 200 μm. (E) 3–4-week-old juvenile removed from tube with feeding tentacle buds (tb) and partially digested food (fo) in the digestive system. Scale bar: 300 μm.

along the ventral surface, whereas this fusion takes place in *Polygordius* at metamorphosis. *Polygordius* undergoes much renewal of esophageal and digestive system tissues, but these tissues remain relatively unchanged in *Owenia*. Wilson (1932) hypothesized that the digestive system in the endolarva of *Polygordius* is too short prior to metamorphosis for the juvenile worm, requiring growth and rearrangement of these tissues. The digestive system of *Owenia*, however, appears to be the correct length for the juvenile worm. These differences in structures and sequence of events may suggest an independent evolution of "cataclysmic" metamorphosis in two groups whose larval resemblance is coincidental rather than evolutionary.

This study of embryogenesis and larval development in *Owenia collaris* reveals both conservation and extreme modification. The unique mitraria larva represents a remarkable departure from the stereotypical annelid trochophore. It is as much diverged from the spiralian stereotype as the nemertean pilidium, with which *Owenia*'s development indeed shares some traits, including enlarged first quartet micromeres, gastrulation by invagination into a large blastocoel, and the formation of a convoluted primary ciliated band from numerous proliferative cells. Ultimately, the embryo and larva of *Owenia* illustrate that spiralian development is much more plastic than was once thought, and that developmental traits once considered diagnostic for, and even defining to, the deuterostomes can arise convergently.

Acknowledgments

Thanks to S. A. Maslakova for the use of her confocal microscope, and to the Friday Harbor Labs for providing research space for T.I.S. Comments by R. B. Emlet, C. M. Young, S. A. Maslakova, and two reviewers greatly improved this manuscript. The National Science Foundation

supported this research through a GK-12 fellowship (#0338153) to T.I.S. and grants to C. M. Young and R. B. Emlet (OCE-100548) and R. B. Emlet (OCE-9911682). G. von D. was supported by NIH grant # 066050 to G. M. Odell.

Literature Cited

Aguinaldo, A. M. A., J. M. Turbeville, L. S. Linford, M. C. Rivera, J. R. Garey, R. A. Raff, and J. A. Lake. 1997. Evidence for a clade of nematodes, arthropods and other moulting animals. *Nature* **387:** 489–493.

Aguinaldo, A. M. A., and J. A. Lake. 1998. Evolution of the multicellular animals. *Am. Zool*. **38:** 878–887.

Aiyar, R. G. 1931. Development and breeding-habits of a polychaete (*Marphysa*). *J. Linn. Soc. Lond.* **37:** 387.

Akesson, B. 1967. The embryology of the polychaete *Eunice kobiensis*. *Acta Zool*. **49:** 141–192.

Anderson, D. T. 1959. The embryology of the polychaete *Scoloplos armiger*. *Q. J. Microsc. Sci.* **100:** 89–166.

Bartolomaeus, T. 1995. Secondary monociliarity in the Annelida: monociliated epidermal cells in larvae of *Magelona mirabilis* (Magelonida). *Microfauna Mar*. **103:** 27–332.

Blake, J. A. 2000. Chapter 5. Family Oweniidae Rioja, 1917. Pp. 97–127 in *Taxonomic Atlas of the Benthic Fauna of the Santa Maria Basin and the Western Santa Barbara Channel.* Vol. 7. *The Annelida* Part 4*: Polychaeta: Flabelligeridae to Sternaspidae*, J. A. Blake, B. Hilbig, and P. V. Scott, eds. Santa Barbara Mus. Nat. Hist., Santa Barbara, CA, 348 pp.

Bourlat, S. J., C. Nielsen, A. D. Economou, and M. J. Telford 2008. Testing the new animal phylogeny: a phylum level molecular analysis of the animal kingdom. *Mol. Phylogenet. Evol.* **49:** 23–31.

Costello, D. P. 1945. Experimental studies of germinal localization in *Nereis*. I. The development of isolated blastomeres. *J. Exp. Zool*. **100:** 19–66.

Damen, P., and W. J. A. G. Dictus. 1994. Cell lineage of the prototroch of *Patella vulgata* (Gastropoda, Mollusca). *Dev. Biol.* **162:** 364–383.

Dautert, E. 1929. Die Bildung der Keimblätter bei Paludina. *Zool. Jahrb. Anat.* Vol. 50.

Emlet, R. B., and R. R. Strathmann. 1994. Functional consequences of simple cilia in the mitraria of Oweniids (an anomalous larva of an anomalous polychaete) and comparisons with other larvae. Pp. 143–157 in *Reproduction and Development of Marine Invertebrates*, W. H. Wilson, S. A. Stricker, and G. L. Shinn, eds. Johns Hopkins University Press, Baltimore.

Fernando, W. 1931. The origin of the mesoderm in the gastropod *Viviparus* (=*Paludina*). *Proc. R. Soc. Lond. B* **107(752):** 381–390.

Gardiner, S. L. 1978. Fine structure of the ciliated epidermis on the tentacles of *Owenia fusiformis* (Polychaeta, Oweniidae). *Zoomorphologie* **91:** 37–48.

Gardiner, S. L. 1979. Fine structure of *Owenia fusiformis* (Polychaeta, Oweniidae) and its significance for annelid phylogeny. Ph.D. dissertation, University of North Carolina at Chapel Hill.

Hartman, O. 1969. *Atlas of the Sedentariate Polychaetous Annelids from California.* Allan Hancock Foundation, University of Southern California, Los Angeles.

Koh, B. S., and M. R. Bhaud. 2003. Identification of new criteria for differentiating between populations of *Owenia fusiformis* (Annelida Polychaeta) from different origins: rehabilitation of old species and erection of new species. *Vie Milieu* **53:** 65–95.

Maslakova, S. A., M. Q. Martindale, and J. L. Norenburg. 2004. Vestigial prototroch in a basal nemertean, *Carinoma tremaphoros* (Nemertea; Palaeonemertea). *Evol. Dev*. **6:** 219–226.

Nielsen, C. 2001. *Animal Evolution: Interrelationships of the Living Phyla.* 2nd ed. Oxford University Press, New York.

Nielsen, C. 2004. Trochophora larvae: cell-lineages, ciliary bands, and body regions. 1. Annelida and Mollusca. *J. Exp. Zool*. **302B:** 35–68.

Okada, K. 1970. Chapter 7: Annelida. Pp. 192–241 in *Invertebrate Embryology*, M. Kume and K. Dan, eds. Bai Fu Kan Press, Tokyo.

Peterson K. J., and D. J. Eernisse. 2001. Animal phylogeny and the ancestry of bilaterians: inferences from morphology and 18S rDNA gene sequences. *Evol. Dev.* **3:** 170–205.

Rattenbury, J. C., and W. E. Berg. 1954. Embryonic segregation during early development of *Mytilus edulis*. *J. Morphol*. **95:** 393–414.

Render, J. A. 1982. A demonstration of the inhibitory influence over apical tuft formation by the second polar lobe of the *Sabellaria cementarium* embryo. Ph.D. dissertation, University of Texas at Austin.

Rouse, G. W. 1999. Trochophore concepts: ciliary bands and the evolution of larvae in spiralian Metazoa. *Biol. J. Linn. Soc.* **66:** 411–464.

Rouse, G. W., and K. Fauchald. 1997. Cladistics and the polychaetes. *Zool. Scr.* **26:** 139–204.

Rouse, G. W., and K. Fauchald. 1998. Recent views on the status, delineation and classification of the Annelida. *Am. Zool*. **38:** 953–964.

Schroeder, P. C., and C. O. Hermans. 1975. Annelida: Polychaeta. Pp. 1–213 in *Reproduction of Marine Invertebrates*, Vol. 3, A. C. Giese and J. S. Pearse, eds. Academic Press, New York.

Shankland, M., and R. M. Savage. 1997. Annelids, the segmented worms. Pp. 219–235 in *Embryology: Constructing the Organism,* S. F. Gilbert and A.M. Raunio, eds. Sinauer, Sunderland, MA.

Smith, P. R. 1981. Larval development and metamorphosis of *Sabellaria cementarium* Moore (Polychaeta: Sabellariidae). Ph.D. dissertation, University of Alberta, Edmonton.

Smith, P. R., E. E. Ruppert, and S. L. Gardiner. 1987. A deuterostome-like nephridium in the mitraria larva of *Owenia fusiformis* (Polychaeta, Annelida). *Biol. Bull*. **172:** 315–323.

Strathmann, M. F. 1987. *Reproduction and Development of Marine Invertebrates of the Northern Pacific Coast: Data and Methods for the Study of Eggs, Embryos, and Larvae*, pp. 138–195. University of Washington Press, Seattle, WA.

Thompson, T. E. 1960. The development of *Neomenia carinata* Tullberg. *Proc. R. Soc. Lond. B Biol. Sci.* **153:** 263–278.

Wilson, D. P. 1932. On the mitraria larva of *Owenia fusiformis* Delle Chiaje. *Philos. Trans. R. Soc. Lond. B Biol. Sci.* **221:** 231–334.

Winesdorfer, J. E. 1967. Marine annelids: *Sabellaria*. Pp. 157–162 in *Methods in Developmental Biology*, F. M. Wilt and N. K. Wessells, eds. Crowell, New York.

Woltereck, R. 1902. Trochophora-Studien I. Histogie der larve und die Entstehung des Annelids bei den Polygordius-Arten der Nordsee. *Zoologica (Stuttg.)* **13 (34):** 1–71.

Zardus, J. D., and M. P. Morse. 1998. Embryogenesis, morphology and ultrastructure of the pericalymma larva of *Acila castrensis* (Bivalvia: Protobranchia : Nuculoida). *Invertebr. Biol.* **117:** 221–244.

Zimmer, R. L. 1964. Reproductive biology and development of Phoronida. Ph.D. dissertation, Univ. of Washington, Seattle. 416 pp.